Figure 1. Abundance-driven vs. observed change

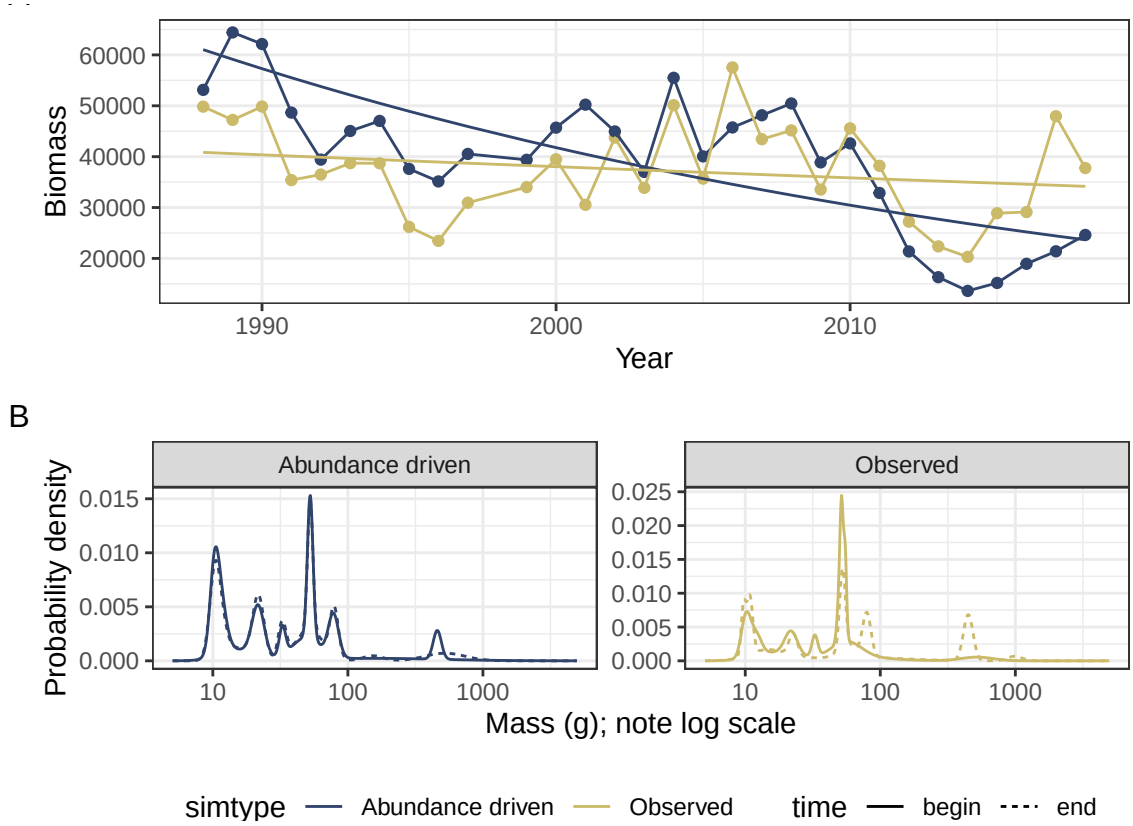

Figure 1. Illustration of abundance-driven (null model) dynamics as compared to observed dynamics (A), and the underlying dynamics of the ISD (B) for a sample route (LINDBROOK, Alberta). **A. Dynamics of total biomass.** The gold points show the true values for total biomass in each year, and the blue points show the values for total biomass simulated from a null model that incorporates change in total abundance, but assumes no change in the size structure, over time. The smooth lines show the predicted values from a Gamma (log-link) linear model of the form `total_biomass ~ year * simtype`. For this route, change in the individual size distribution has decoupled the dynamics of biomass from those that would occur due only to changes in abundance. The slope for abundance-driven dynamics is significantly more negative than for the observed dynamics (interaction term p = 0.0013), which do not have a slope significantly different from zero (slope term p = .27). **B. Underlying changes in the ISD.** The individual size distributions for the first 5 years (solid lines) and last 5 years (dashed lines) of the timeseries. The x-axis is body size (as mass in grams; note log scale) and the y-axis is probability density from a Gaussian mixture model fit to a vector of simulated individual masses for all individuals observed in the years in questions, standardized to sum to 1. For the abundance-driven (blue) scenario, individuals' species identities (which determine their body size estimates) are re-assigned at random weighte by each species' mean relative abundance throughout the timeseries, resulting in a consistent individual size distribution over time. For the observed (gold) scenario, individuals' body sizes are estimated based on their actual species identities. For this route, species composition has shifted over time and produced different ISDs for the "begin" and "end" time periods. Specifically, the "end" ISD has peaks at larger body sizes (ca. 90g and 500g) not present in the "begin" ISD. This redistribution of density towards larger body sizes results in an overall increase in body size community wise, which partially offsets declines in total biomass from those expected given change in abundance alone.

Figure 2. Directions and magnitudes of change.

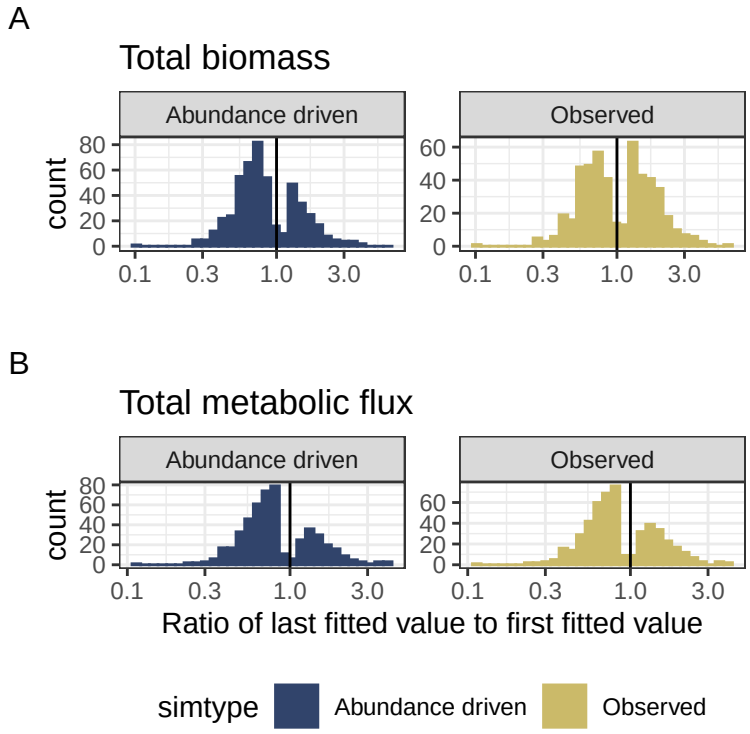

Figure 2. Long-term trends in total biomass and energy use Histograms showing the direction and magnitude of change over time for the abundance-driven (left) and observed (right) changes in biomass (A) and energy use (B), for communities with a significant slope and/or interaction term (for biomass, 500/739 routes; for energy use, 509/739 routes). Change is summarized as the ratio of the fitted value for the last year in the time series to the fitted value for the first year in the timeseries from the best-fitting model for that community. Values greater than 1 (vertical black line) indicate increases in total energy or biomass over time, and less than 1 indicate decreases. The abundance-driven dynamics (left) reflect the trends fit for the null model, while the observed dynamics (right) reflect trends incorporating both change in total abundance and change in the size structure over time. For communities with no significant interaction term in the best-fitting model, the "abundance-driven" and "observed" ratios will be the same; interaction terms will result in different ratios for "abundance-driven" and "observed" dynamics.

Among routes with temporal trends, there are qualitatively different continental-wide patterns in abundance-driven and observed dynamics for total biomass and total metabolic flux. 70% of trends in abundance-driven dynamics for energy use are decreasing, and 67% for biomass. However, for biomass, observed dynamics are balanced evenly between increases (49% of routes) and decreases (51%) - indicating that changes in the size structure produce qualitatively different long-term trends for biomass than would be expected given abundance changes alone. However, trends for energy use (which scales nonlinearly with biomass) are dominated by decreases (35% of routes), more closely mirroring the trends expected given changes in abundance.

Tables: Model outcomes

Table 1.

Currency	Selected model	Number of routes	Proportion of routes
Total biomass	Intercept-only	239	0.32
Total biomass	Trend, not decoupled	351	0.47
Total biomass	Decoupled trend	149	0.20
Total metabolic flux	Intercept-only	230	0.31
Total metabolic flux	Trend, not decoupled	456	0.62
Total metabolic flux	Decoupled trend	53	0.07

Table 1. Selected models. Table of the number and proportion of routes whose dynamics for total biomass and total energy use are best-fit by: a model with no temporal trend (intercept-only model, `response ~ 1`); a model with a temporal trend, but no difference in trend between observed and abundance-driven dynamics (`response ~ timeperiod`); or a model with decoupled temporal trends for observed and abundance-driven dynamics (`response ~ timeperiod * source`).

For 31-32% of routes, models with trends do not outperform simple intercept-only models. For the remaining routes, in most instances, the dynamics of biomass and energy use exhibit a temporal trend, but with no detectable difference in the temporal trends for abundance-driven and observed dynamics. However, for a substantial minority of routes (20% overall for biomass, or 30% of routes with a temporal trend; 7% overall for energy use, or 10% of routes with a temporal trend), there is a detectable deviation between the trends expected due only to changes in abundance and the observed dynamics.

Figure 3. Visualizing decoupling

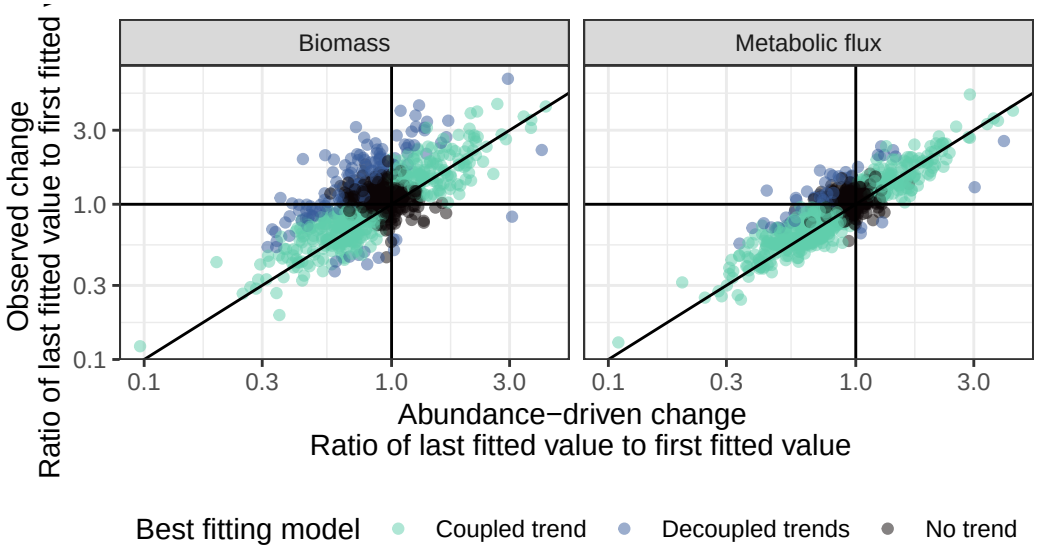

Figure 4. How the ISD contributes to decoupling

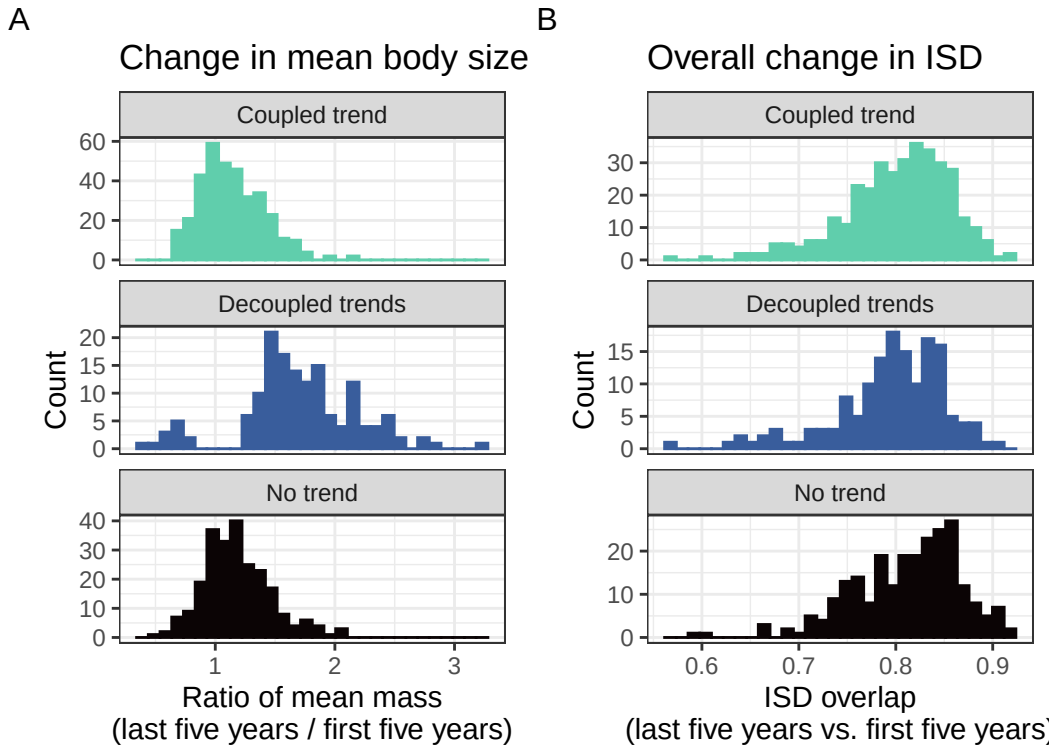

R2 of binomial GLM `overlap ~ model_formula` (which does not beat a `overlap ~ 1` via AIC, FYI)

References